STRAY CURRENT DESIGN PARAMETERS FOR DC RAILWAYS

J.G.Yu Student Member, IEEE C.J.Goodman M.A Ph.D C.Eng MIEE.

School of Electronic and Electrical Engineering
University of Birmingham,
PO BOX 363, Birmingham, B15 2TT, U.K.

Abstract: In this paper, two objective parameters concerning the potential damage due to stray currents from DC railways are proposed. These are the total stray current (as a function of time), and the gross electric charge leaked from the railway during a period of time. These two parameters can serve as an indication of the extent of the stray current problem. Computer simulation methods for obtaining these parameters are also presented. Some results are obtained and analysed.

1. Introduction

DC powered electric railways are widely used for urban transportation, usually in the voltage range of 600 to 1500 volts. Very often, the running rails are used as the return conductor for traction current, in addition to their main function of supporting the trains. Due to this arrangement, two problems are created, namely, the rail potential rise, or touch and step voltage problem and the corrosion problem. The two problems are interrelated. This paper is mainly concerned with the corrosion problem. The touch and step voltage problem will be addressed in a future paper.

Normally, all the running rails that are used as the return conductor are bonded together regularly so that these rails carry the return current evenly. Since the rails have the same potential in the same cross section, they can be treated as a single conductor when dealing with the leakage current problem.

Take a simple static feeding situation as an example, as shown in Fig.1 (a). The longitudinal rail resistance exhibited to the return current causes a voltage drop, between the two points T and S, where the current enter and leaves the rails respectively.

Due to the imperfect insulation between the rails and the surrounding ground, there is a current exchange between them, therefore, the rails exhibit a potential with respect to the remote ground. Assume that the rail-ground conductance is uniform in the section, the rail potential profile is shown in Fig.1 (b).

The current exchange between the rails and the ground is described by a current density function $\delta(x)$ against position x. This is shown in Fig.1 (c). In the rail section (l/2,l), current leaves the rails to enter the ground. This is the leakage current. In the section(0,l/2),the leaked current leaves the ground to enter the rails. $\delta(x)$ is called the leakage current density. Here, the end effects of the rails are neglected.

In the ground, the leaked current is known as the stray current, together with stray currents generated from other sources to the ground. Therefore, the DC railways are a source of stray current.

As is well known, stray currents cause corrosion. The stray current generated by a DC railway may cause corrosion to buried metallic facilities within its sphere of influence, as well as causing corrosion to the rails themselves. In engineering practice, it is highly desirable to design a railway system that fulfils its functions, and at the same time, to cause no damage or minimum damage to useful facilities.

The corrosion problem has been a major concern to the railway and other parties involved since the early days of DC railways [2]. Various measures have been adopted by the railway authorities to overcome this problem. There has been a renewed concern over this problem, with a recent upsurge of interest in the urban rapid transit systems ([3] to [17]).

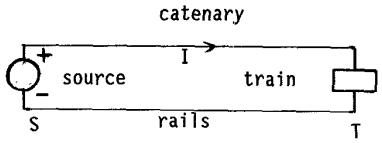

(a). Loading condition

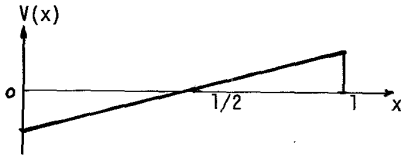

(b). Rail potential

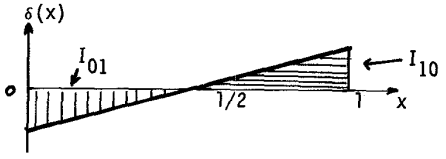

(c). Leakage current density

Fig.1 Schematic diagrams for a simple feeding section

However, due to the lack of detailed data, it is very difficult to compare the merits of different approaches to the problem on a scientific basis. In the past, designs had to be based on experience accumulated over a long period of railway construction and operation.

In this paper, two objective parameters concerning the potential damage due to stray currents are proposed. These are the total stray current (as a function of time), and the gross electric charge leaked from the railway on a hourly, monthly or annual basis. These two parameters can serve as an indication of the extent of the stray current problem. They can be obtained from computer simulations based on detailed modelling of the earthing and conductor configurations and the operational conditions, using a specially developed stray current analysis module, linked to an existing double-track, multi-train movement and power supply simulator.

2. Proposed Design Parameters for Stray Current

2.1 Faraday's Law

In a corrosion cell, the relationship between the amount of metal that reacts and the charge Q that causes the reaction is described quantitatively by Faraday's Law [1]:

$$m = kQ \qquad (1)$$

where m is the weight of metal decomposed (grams) and k is the electrochemical equivalent of the metal in grams/coulombs. If the charge is produced by a constant current I over a period of time t, then, Q=It, and

$$m = kIt \qquad (2)$$

In this case, the constant k may be expressed in the more popular term, kg/Ampere/year, i.e., the annual corrosion rate in kg by applying one Ampere of constant current. A few values of k for different metals are listed in Table 1.

2.2 Total Stray Current

Definition of total stray current

Given the simple static situation shown in Fig.1 (a), and the leakage current density function in Fig.1 (c), in section (1/2,1), current leaks to the ground. Let the rails be designated as conductor 1. By integrating the current density function over this section, the total current leaked to the ground is obtained as I_{10}.

Similarly, in section (0,1/2), the leaked current is picked up by the rails. The total current picked up by the rails is I_{01}. According to Kirchhoff's Current Law, the total current leaked to the ground is equal to the total current that is picked up from the ground, or

$$I_{01} = I_{10} \qquad (3)$$

Table 1

Type of Metal	k (kg/Ampere/year)
Aluminium	2.93
Iron	9.12
Zinc	10.69
Copper	26.6

The leaked current in the ground is the stray current. The total amount of the current leaked to the ground is defined as the total stray current (TSC).

When the substation ground is connected to the rails, the leakage pattern is different. Further, when more trains and substations are involved, the situations become more complicated. But the same principle applies. That is, some parts of the rails leak current, other parts pick up the leaked current. This is abstractly shown in Fig.2.

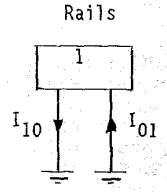

Fig.2 Total leakage current from the rails

The total stray current can be obtained by using computer simulation, which is described in the following section.

Stray Current Collection Mats

In some DC railway systems, concrete slabs are used to support the rails, instead of wood or concrete sleepers. The concrete slabs are reinforced with reinforcing bars (rebars for short). These slabs are manufactured in the works or built on site, typically 50 meters long for each section. Within each section, the rebars are bonded together to form an electrical entity, called a rebar mat. There is no electrical connection between rebar mats of different slab sections.

In practice, the electrical power supply engineers have tried to use the rebars in the concrete slabs to collect the leakage currents, in collaboration with the civil engineers. In such installations, a separate "fault current return" (FCR) conductor is used (also referred to as the "traction earth conductor"). The return conductor itself is insulated from the rails and ground. It leads to the negative terminal of the source via a diode.

The concrete is the first conduction medium for leakage currents from the rails. By connecting the rebars in each section of the slab to the FCR, it is intended that a substantial part of the leakage current should follow the path of the FCR. In this way, the rebar mats are used as leakage current collection mats, in addition to their structural

functions. The electrical connections are schematically shown in Fig.3 (a).

The effectiveness of such schemes depends on the factors that affect the rebar-earth resistance, the rail-earth resistance and the rail-rebar resistance, such as weather conditions.

The rebar mats and the FCR can be treated as a single conductor, with appropriate parameters. The interchange of current between the rails (labelled as conductor 1) and the rebars (labelled as conductor 2) in a section are schematically shown in Fig.3 (b). The total stray current is $(I_{10}+I_{20})$. Obviously,

$$I_{01}+I_{02} = I_{10}+I_{20} \qquad (4)$$

Total Stray Current as an Objective Parameter

As is understood, the total stray current is involved with the corrosion of the rails themselves. If a buried pipeline is within its sphere of influence, part of the stray current may be picked up by the pipeline. Those parts of the pipeline that are made anodic by the stray current are subject to corrosion. The areas made cathodic by the stray current are protected against corrosion. The part of the stray current that does not enter the pipeline is harmless to the pipeline.

Even when there is no stray current generated by railways in the vicinity of the pipeline, the pipeline still corrodes due to electrochemical action. When the stray current is present, it acts as an accelerating factor for the natural pipeline corrosion. It is similar for any other buried metallic structures.

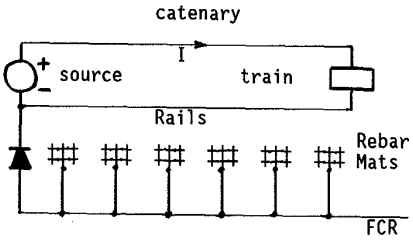

(a). Schematic showing the use of rebars as stray current collection mats

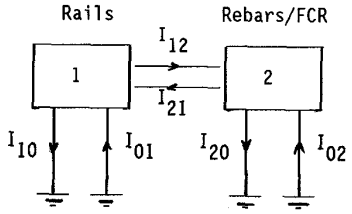

(b). Total leakage current from the rails and the rebar/FCR

Fig.3 The use of rebar mats for stray current collection

In practice, the exact distribution of stray current in the ground is extremely complicated and difficult to analyse and quantify. The total stray current is easier to obtain from computer simulation. Therefore, it is proposed that total stray current should be used as an objective parameter, which serves to indicate the extent of the leakage current problem.

Total Stray Current as a Function of Time

For an operational railway system, the train positions are varying at different times and the total demand on power supply is changing, which results in changes of train and substation current and consequently the leakage current. The value of total stray current thus varies with time. By observing the total stray currents over a period of time, a function of total stray current against time may be obtained. This is schematically shown in Fig.4.

2.3 Gross Leakage Charge

Refer to the total stray current function, as shown in Fig.4. Let i(t) denote the total stray current from a DC railway at time instant t. An integration between t1 and t2 gives the total charge delivered by the DC railway to the ground

$$Q = \int_{t1}^{t2} i(t)\, dt \qquad (5)$$

This charge is defined as the gross leakage charge (GLC) that is emitted from the railway to ground during the time interval (t1,t2). According to Faraday's Law, the weight of corroded metal from the rails is directly proportional to this charge.

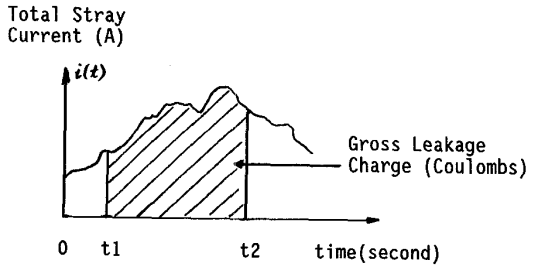

Fig.4 Total Stray Current as a Function of Time

As it happens, part of this charge may also be involved in the corrosion process of other buried metal works, although it is very difficult to find out what proportion of the gross leakage charge actually damages such metal works, as this depends on a lot of factors.

Since the GLC is easier to obtain, it is proposed that it should be used as an objective parameter in the evaluation of stray current emission from a DC railway.

When a DC railway is being designed, a lot of factors affect the leakage current. Such factors are the system voltage level, substation spacing, system earthing condition, rail resistance, track gradients, rail insulation and so on. When a railway is under

operation, the operational conditions also affect leakage current. Such factors are traffic density, vehicle loading conditions, driving system characteristics, and so on.

It is intended that the objective parameters may be used to compare leakage current for different system and operational conditions. The following section describes the computer analysis model to obtain these parameters.

3. Computer Simulation Model

The computer simulation model consists of two major parts: a transmission line analysis model and a multi-train simulator. These are explained as follows.

3.1 Transmission Line Model

Assume that the longitudinal resistance and leakage conductance of the rail are given. Assume also that at a certain instant of time, the railway system loading condition is given, that is, the train positions, train currents and substation currents are known. Then the rail-earth system can be treated as a transmission line under shunt energisation at multiple points [18], as shown in Fig.5 (a).

The transmission line can be best solved digitally by taking into account of the nonuniformity of the rail parameters and the earthing and bonding conditions. If the rebar mats and other conductors are involved, a transmission line system is formed, which can be solved by using multi-conductor theory [19]. A schematic diagram for the multi-conductor model is shown in Fig.5 (b).

Detailed modelling methods for the single conductor model and the multi-conductor model are given in [15] and [16] respectively.

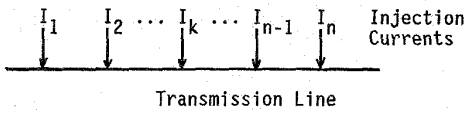

(a). A transmission line with distributed parameters under shunt energisation

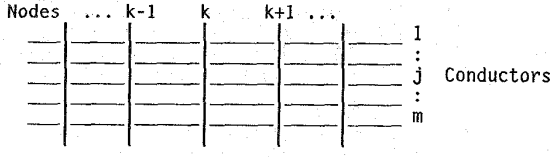

(b). A multi-conductor system

Fig.5 Circuit models for a single transmission line and a multi-conductor system

3.2 The Multi-Train Simulator

A multi-train simulator has been developed in the University of Birmingham in the last two decades. It has been extensively used as a design aid to study the operational conditions of train movement and performance, and the traction power supply network conditions in both mainline and urban transit railway systems [20][21][22]. Detailed treatment of the simulator is outside the scope of this paper. A brief description suffices for the purpose of understanding the stray current analysis package.

The simulator consists of two major modules functionally: a train movement module and a power network module. The movement module itself consists of two parts: part A and part B. The main function of the simulator is to assemble the two modules to simulate the dynamic interaction of the train movement and the condition of the power supply system. The flow chart of the simulator is shown in Fig.6.

The movement simulator is time based and it is assumed that time proceeds in discrete steps: typically of one second. In each time step, the power network status is steady, and the train accelerations are constant.

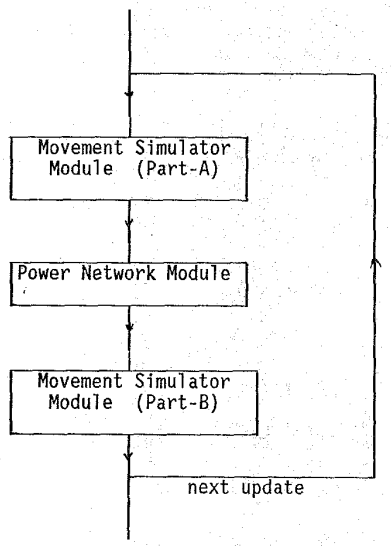

Fig.6 Flow Chart for the Multi-Train Simulator

Movement Module Part-A: The movement simulator part-A establishes train modes. The possible operation modes are: motoring, braking, coasting and waiting. It is assumed that at the start of each update interval, the positions and velocities of all trains are known.

Power Network Module: Using the information of train position, velocity, operational mode and last known voltage for each train, an approximate linear network is derived for the whole electrical network consisting of substations, trains, and supply conductors. The resulting network is solved and the results checked against nonlinear constraints which represent nonreceptive conditions at each substation and an overvoltage limit in regeneration on each braking train. This process is repeated until all system constraints are satisfied. The final solution enables the energy consumption for the current update

interval to be deduced and a new voltage at each train to be assigned.

Movement Module Part-B: When the voltage at each train is known, the train performance may be calculated from the mode, velocity and last known voltage using movement simulator part-B. This is done for each train and the new train positions are updated.

Once the calculations for the existing update interval are complete, the process can be restarted for the next update interval.

3.3 The Integrated Model

The integration of the multi-train simulator and the multi-conductor model makes it possible to study the leakage current problem in more detail. The two objective parameters of total stray current and the gross leakage charge in a DC railway system can be evaluated. The flow chart for the integrated simulation model is shown in Fig.7.

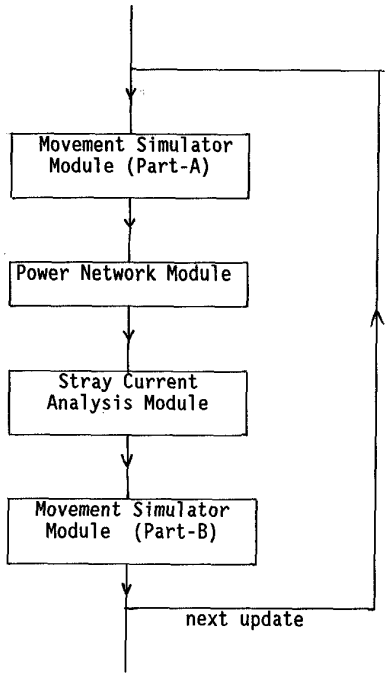

Fig.7 Flow Chart for the Integrated Simulation Model

3.4 One Hour's Equivalent Gross Leakage Charge

Summations The simulation performance is done over a period of time, e.g. from t1 to t2. Because the digital simulation is performed in discrete time steps, the gross leakage charge has to be obtained approximately by summations over the discrete time intervals. During each interval the total stray current is regarded constant. The shorter the time interval chosen, the more accurate the representation. The summation is described by the following expression:

$$Qx = \sum_{t1}^{t2} i(t)\Delta t \qquad (6)$$

In practice, one simulation performance may be done over a period of time that is different from another. In order to make the results comparable, the equivalent GLC over 1 hour's time is defined.

Let the duration of simulated time be Tx (seconds), Tx=t2-t1, and the corresponding GLC be Qx (Ampere-seconds, or Coulombs), then the equivalent GLC over 1 hour's time (Qh) is

$$Qh = 3600.Qx/Tx \quad \text{(in Coulombs)} \qquad (7a)$$

or

$$Qh = Qx/Tx \quad \text{(in Ampere-hours)} \qquad (7b)$$

In practical operation of a DC railway line, different service conditions (e.g., different headways) may be used at different times for one day's service. For example, in a rapid transit system, a shorter headway in peak hours and a longer headway in off-peak hours is usual. Such conditions can be simulated by having several simulation performances, and the equivalent GLC over 24 hours derived. Ultimately, an annual equivalent GLC can be derived, by taking into account seasonal variation of basic parameters, such as rail-ballast resistances, earthing resistances, and so on.

4. Results and Discussions

The results are presented in two parts in this section: the static results and the dynamic results. The static results are obtained for a fixed frame picture under some assumed loading conditions. The dynamic results are obtained by using the integrated model to simulate a railway system under practical operational conditions. Emphasis is given to system earthing conditions.

4.1 Static Results for the Total Stray Current

To obtain some simulation results for the total stray current in the static situation, a section of test track is used. The test track is an 8 km long, double-track railway line. This is illustrated in Fig.8. There are three substations on the line, namely, SS1, SS2, SS3. Each substation has an 1 ohm ground. In the SS3 area, a depot is connected to the line. The input resistance of the depot seen looking from the rails at 8 km in the dry condition is 0.08 ohm. In the wet condition it is 0.025 ohm.

The longitudinal rail resistance is 8 milli-ohm/km (4 rails in parallel with regular bonding). Two types of rail support structures are used: ballast with wood sleepers for ground level and concrete sleepers for aerial structures. These structures are used in a mixed pattern. Table 2 lists the location of each structure.

Table 2

section number	end position of section(m)	type of sleeper
1	2215.4	wood
2	3384.6	concrete
3	5169.2	wood
4	5784.6	concrete
5	6461.5	wood
6	8000.0	wood

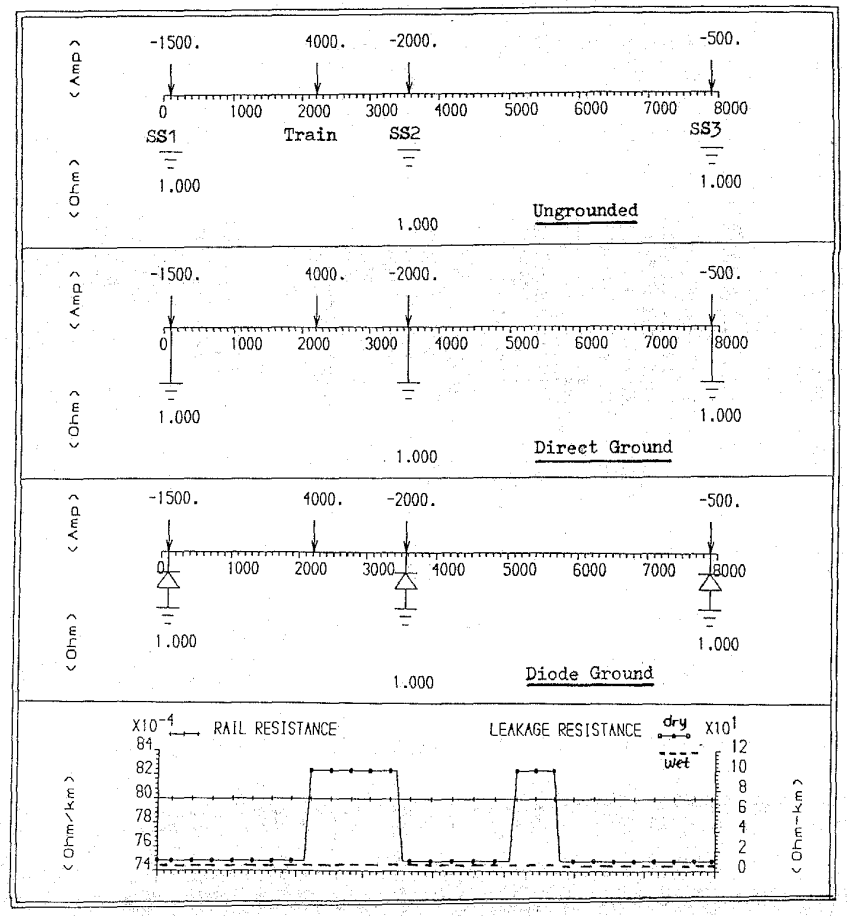

Fig. 8 Schematic diagram for an 8 km line

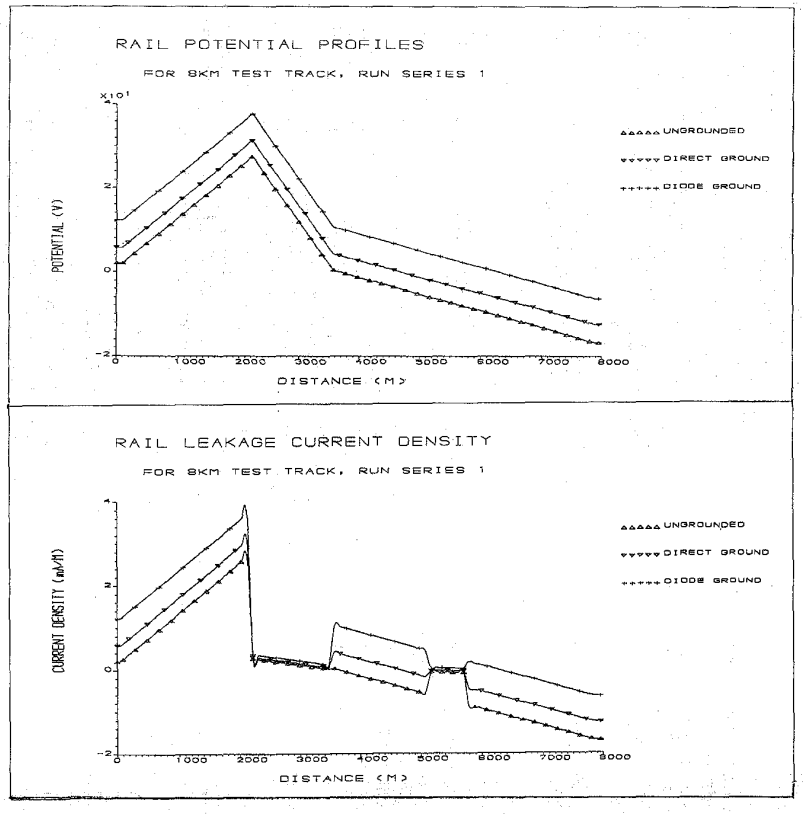

Fig. 9 Rail potential and leakage current densities for the 8 km line

The rail-earth leakage resistance for the two types of structures are different. For the wood sleeper, it ranges between 5 and 10 ohm-km; for the concrete sleepers, it ranges between 5 and 100 ohm-km (4 rails in parallel). These are assumed values. In practice, the rail-earth resistance can be obtained either by site measurement or by theoretical calculations [18].

For the substation grounds, 3 conditions are considered, namely, ungrounded; direct ground and diode ground. There is one starting train with 4000 A current on the track. The 3 substations supply 1500, 2000, 500 A currents respectively. The earthing conditions, loading condition and the rail parameters are all shown in Fig.8.

Test Runs

A number of test runs for this test track are done, in order to observe the results under different conditions. These are classified in 4 series, each series having 3 separate runs.

Series 1: Dry condition, no depot connection. Leakage resistances for the rails are 10 ohm-km for wood, 100 ohm-km for concrete. 3 runs are made by considering different earthing conditions:

run 11: ungrounded;
run 12: direct ground with 1 ohm earth;
run 13: diode ground with 1 ohm earth.

Series 2: Dry condition with depot connection. Other conditions as in series 1. Run numbers 21,22,23, corresponding to runs 11,12,13.

Series 3: Wet condition. Leakage resistances are 5 ohm -km for both wood and concrete. Other conditions as in series 1. Run numbers 31,32,33.

Series 4: Wet condition. Other conditions as in series 2. Run numbers are 41,42,43.

The conditions for the 4 series are listed in Table 3.

Table 3

Series No.	depot connection	track condition
1	no	dry
2	yes	dry
3	no	wet
4	yes	wet

For all the runs, it is assumed that the running rails do not extend beyond the 0 to 8 km section. The rail potential and leakage current densities for run numbers 11,12,13 are shown in Fig.9.

For each run, the total stray currents are derived, and a maximum rail potential is identified. The results are listed in Table 4. The corresponding histograms are shown in Fig.10.

Conclusions

A number of conclusions about the total stray current and the maximum rail potential may be drawn according to the simulation results.

Earthing Conditions: For the total stray current, the ungrounded scheme results in the lowest TSC, the direct-ground scheme results in the highest TSC. The ascending order for different earthing schemes is: ungrounded; diode-ground; direct-ground. This is understandable in that the more connections (bonding) from rail to ground, the higher the leakage current.

For the maximum rail potential, when the depot is not connected to the track, the ungrounded scheme results in the lowest maximum-potential and the diode ground results in the highest maximum-potential. The ascending order is: ungrounded; direct-ground; diode-ground. If the depot is connected to the track, the direct-ground scheme results in the lowest maximum-potential. The ungrounded and the diode-ground schemes give almost the same maximum potential.

Table 4

Run No.	Max. positive potential (V)	Max. Negative potential (V)	Max. Transferred Potential (V)	Total Stray current (A)
11	27.4	-16.84	44.28	3.328
12	31.3	-12.54	43.80	14.509
13	37.7	-6.42	44.11	7.001
21	43.2	-0.80	44.01	9.890
22	40.2	-2.70	42.94	36.297
23	43.3	-0.74	44.01	9.923
31	25.7	-18.36	44.11	8.849
32	29.8	-13.84	43.63	19.075
33	31.0	-12.70	43.73	17.106
41	42.6	-0.71	43.33	27.387
42	40.9	-1.37	42.23	54.413
43	42.6	-0.69	43.33	27.412

Depot Connection: The depot acts as a low resistance ground. Connection of the depot to the track results in higher leakage current.

Under this condition, the maximum-potential is also increased significantly under each earthing condition.

Rail-Earth Leakage Resistances: A lower rail-earth resistance (or higher conductance) increases leakage current significantly.

On the other hand, a lower rail-earth resistance only reduces the maximum-potential marginally.

Maximum Transferred Potential: The maximum transferred rail potential is mainly governed by the longitudinal rail resistance and the current carried through it. Since the TSC is only a small proportion of the traction return current in any case, the maximum transferred potential is not significantly affected by earthing conditions nor by leakage resistance.

4.2 Dynamic Results for the Gross Leakage Charge

To obtain some dynamic results, the practical data for an operational double track rapid transit railway line is used. The track length is 17 km, with 7 substations and 15 passenger stations. Each substation has a ground resistance of 1 ohm. Using an 120 second headway, the electrical solutions are obtained from 1700 to 1820 seconds. Fig.11 shows the total stray current and maximum rail potential against time.

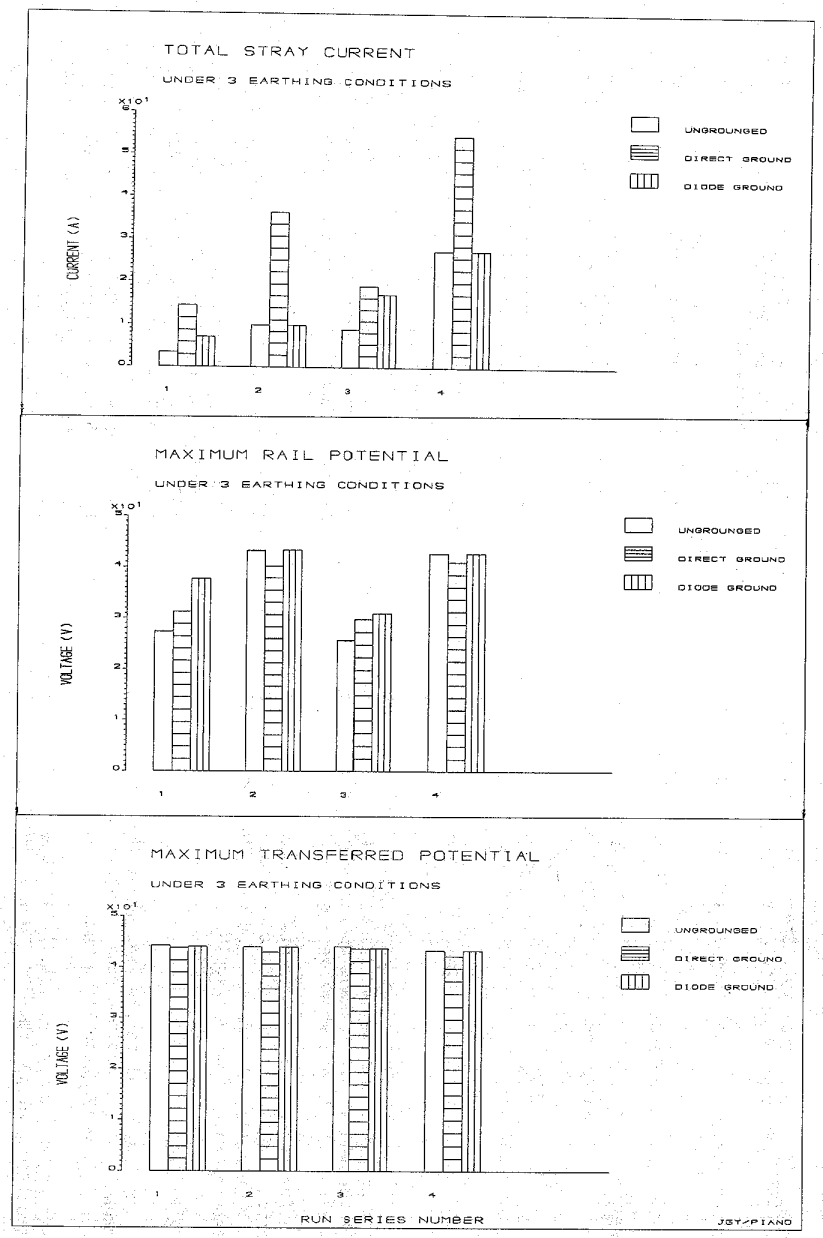

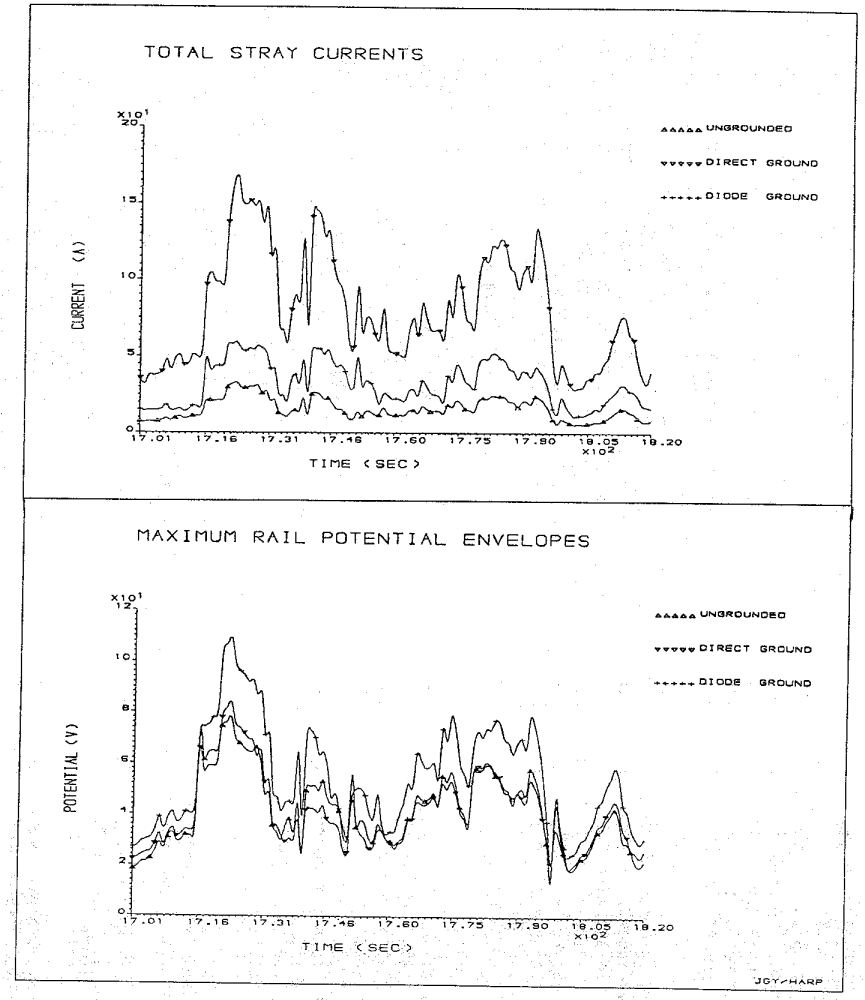

Fig. 10 Histograms for the total stray current, maximum rail potential and maximum transferred potential for the 8 km line (Left)

Fig. 11 Total stray current and maximum rail potential against time for the 17 km line (Top)

For each run, an overall maximum value is identified for the maximum potential, the maximum transferred potential and the maximum total stray current, over the whole period of time simulated. The results are summarised and listed in Table 5. The results confirm the conclusions drawn from the static results.

Table 5

Earthing conditions	Un-grounded	Direct ground	Diode ground
Grand Max. rail potential (V)	78.10	83.94	108.94
Grand Max. transferred rail potential (V)	147.53	142.26	145.20
Grand Max. total stray current (A)	32.91	167.74	59.26
1 hour's equivalent gross leakage charge (ampere-hours)	15.77	80.78	32.13
Average system loading (MW)	12.09	12.09	12.09

These results merely demonstrate what the simulator can achieve. For brevity, no other results are listed.

Changes in other system parameters, such as system voltage levels, substation spacings, traction motor characteristics, etc., result in changes in the total stray current function and the gross leakage charge. Different operational conditions, e.g., traffic density, headway control, will also result in changes in these two parameters.

Having built up this simulation package, a DC railway line can be studied in great detail about its stray current emission, in addition to the acquirement of other useful data. It is hoped that this will enable rational comparison between different designs and operational control strategies.

5. Conclusions

In this paper, two objective parameters concerning the potential damage due to stray currents are proposed. These are the total leakage current (as a function of time), and the gross electric charge leaked from the railway for a certain time duration (e.g. on a hourly or annual basis). These two parameters can serve as an indication of the extent of the stray current problem.

Computer simulation methods for obtaining these parameters are also presented.

Simulation results show that when there is no other intentional connection between the rails and the general ground, the ungrounded scheme performs better than the diode-ground scheme and the direct-ground scheme in terms of the two proposed parameters. Additionally, the results show that the ungrounded scheme is the best choice for controlling touch and step voltages.

However, it is recognised that other factors, such as safety under fault conditions, may preclude the use of an ungrounded arrangement.

6. Acknowledgement

One of the authors, J.G.Yu, is grateful for financial support from GEC-Alsthom Transmission and Distribution Projects Ltd., Stafford, England. The authors also acknowledge many useful discussions with R.W.Sturland and L.R.Denning of the same Company, but would like to stress that the views expressed in this paper are entirely their own.

7. References

[1] Uhlig,H.H. Corrosion and Corrosion Control - an Introduction to Corrosion Science and Engineering. John Wiley & Sons Inc. 3rd edition, 1985

[2] Edale,J. "Tramway Return Circuit - Methods of Handling a Difficult Problem", Transport World, April, 1945.

[3] Takihara,M. "On Stray-Current Corrosion", Quarterly Report, JNR Technical Research Centre, 1971, vol.12, No.2, pp61-67.

[4] Bomar,H.E. Dean,R.O. Hanck,J.A. Orton,M.D. Todd,P.L. "Bay Area Rapid Transit System (BART)", Materials Performance, vol.13, DEC. 1974, pp9-17.

[5] Shaffer,R.E. Venugopalan,S.I. "Stray current control in Dade county 'MetroRail' system", IEEE IAS 15th annual meeting, Cincinatti, USA, 1980, pp285-291.

[6] Shaffer,R.E. Fitzgerald,J.H.III "Stray earth current control, Washington DC metro system", Materials Performance, April 1981, pp.9-15.

[7] Kish,G.D. "Control of stray currents in underground DC railway systems", Materials performance, vol.20, Sept. 1981, pp27-31.

[8] Shaffer,R.E. "Design of DC powered rail transit systems to minimize stray currents", Materials Performance, Sept. 1982, pp.17-22.

[9] Blakeley,P.R. "Interference problems and solutions on the Tyne and Wear Metro" Proc. of the ICorrST Corrosion Conference, 1984, pp.105-120.

[10] Vernon,P. "Stray current corrosion control in metros", Proc. Inst. Civil Eng. vol.80, part-1, 1986, pp.641-650.

[11] Allen,M.P. Ames,D.W. "Interaction and stray current effects on buried pipelines: six case histories", contained in book: "Cathodic Protection - theory and practice", edited by Ashworth,V & Booker,C.J.L. Published by Ellis Herwood Ltd. Chichester, 1986, pp327-343.

[12] Shaffer,R.E. "Stray current control within DC-powered transit systems", Transport Research Record, Vol. 1152, 1987, pp42-48.

[13] Lowes,F.J. "Magnetic observations of earth leakage currents from DC railways", Power Eng. J. Nov. 1987, pp.333-337.

[14] Brunton,L.J. "Earth leakage problems and solutions on the Tyne and Wear Metro", Proc. IEE, vol.136, Pt.B, No.3, May 88, pp.152-160.

[15] Yu,J.G. Goodman,C.J. "Modelling of rail potential rise and leakage current in DC supplied railway systems", Presented to the IEE Colloquium on "Stray Current Effects of DC Railways and Tramways", October, 1990, London.

[16] Yu,J.G. Goodman,C.J. "Computer simulation of stray currents in DC supplied rail transit systems and their corrosive effects", Presented to the IMechE International Conference on Transit 2020, October, 1990, London.

[17] Woodmore,M.J. "Stray Current Mitigation on DC Electrified Railways", Presented to the IMechE International Conference on Transit 2020, October, 1990, London.

[18] Sunde,E.D. "Earth Conduction Effects in Transmission Systems", Dover Publications Inc., New York, 1968

[19] CCITT Study Group 5, Contribution No.54, Chapter 18 and Annex: "Compensating effects of rails, booster transformers and return conductors in the case of alternating current electric traction lines".

[20] Mellitt,B. Goodman,C.J. Arthurton,R.I.M. "Simulator for Studying Operational and Power-Supply Conditions in Rapid Transit Systems", Proc.IEE, vol.125, No.4, 1978, pp.298-303.

[21] Mellitt,B. Goodman,C.J. Arthurton,R.I.M. "Simulation Studies of the Energy Saving with Chopper Control on the Jubilee Line", Proc.IEE, vol.125, No.4, 1978, pp.304-310.

[22] Rambukwella,N.B. Mellitt,B. Goodman,C.J. Mouneimne,Z.S. "Traction Equipment Modelling and the Power Network Simulation for DC Rapid Transit System Studies", IEE conference publication No. 279, September 1987, pp.218-224.